This document is confidential and is proprietary to the American Chemical Society and its authors. Do not copy or disclose without written permission. If you have received this item in error, notify the sender and delete all copies.

Photochemical Hydrogen Evolution from Neutral Water with a Cobalt Metallopeptide Catalyst

Journal:	Inorganic Chemistry
Manuscript ID	ic-2019-02067a.R1
Manuscript Type:	Article
Date Submitted by the Author:	n/a
Complete List of Authors:	Chakraborty, Saikat; University of Rochester, Department of Chemistry Edwards, Emily; University of Rochester, Department of Chemistry Kandemir, Banu; University of Rochester, Department of Chemistry Bren, Kara; University of Rochester, Department of Chemistry; University of Rochester, Department of Chemistry

SCHOLARONE™ Manuscripts

Photochemical Hydrogen Evolution from Neutral Water with a Cobalt Metallopeptide Catalyst

Saikat Chakraborty,[‡] Emily H. Edwards,[‡] Banu Kandemir, Kara L. Bren*

Department of Chemistry, University of Rochester, Rochester NY 14627

‡These authors contributed equally

*email: bren@chem.rochester.edu

Abstract: CoGGH, a Gly-Gly-His tripeptide coordinated to a cobalt ion, is shown to catalyze the reduction of aqueous protons to hydrogen (H_2) in a light-driven reaction in water near neutral pH. Using [Ru(bpy)₃]²⁺ as a photosensitizer and ascorbate as an electron donor, a turnover number up to 2200 with respect to CoGGH has been observed with the system remaining active for more than 48 hours. The reaction conditions that favor H_2 production are consistent with a reductive quenching mechanism. Results also suggest that CoGGH is robust under these reaction conditions and loss of activity over time results from [Ru(bpy)₃]²⁺ degradation.

Introduction

Deriving a carbon-neutral fuel from two of the planet's most abundant resources, water and sunlight, is a response to growing threats from fossil fuel usage. $^{1-3}$ Obtaining energy-dense H_2 by light-driven water splitting (equation 1) is an ultimate goal with inherent difficulties. To perform the full reaction, photochemical systems for water oxidation (equation 2) must be coupled with systems for proton reduction (equation 3). A number of challenges – economic, chemical, and technical in nature – must be met to successfully couple the half-reactions. 3,4

$$H_2O \rightarrow H_2 + 1/2 O_2$$
 $E = -1.23 V$ (1)

$$H_2O \rightarrow 1/2 O_2 + 2 H^+ + 2 e^ E = -0.82 V (pH 7)$$
 (2)

$$2 \text{ H}^+ + 2 e^- \rightarrow \text{H}_2$$
 $E = -0.41 \text{ V (pH 7)}$ (3)

Investigating the water oxidation and reduction reactions separately with the aid of a sacrificial oxidant or reductant has been a valuable strategy for catalyst and system development.⁵⁻⁷ Herein, focus is placed on the proton reduction reaction. Concentrating on half of the system does not lessen the need for scrutiny through the lens of sustainable design. To that end, hydrogen production should also limit unnecessary additives, utilize smart atom economy, and feature clean and simple catalyst syntheses.^{3,8}

In recent years, hydrogen evolution catalyst development has focused on use of base metals, which are relatively abundant and have relatively low toxicity. Many iron, nickel, molybdenum, and cobalt catalysts have been reported, with cobalt as the most frequently chosen metal center (examples are listed in Tables S1 and S2, with an emphasis on those that function in water). $^{6.7,9-12}$ Cobaloxime-type complexes, $^{13-15}$ cobalt polypyridyls, $^{11,14,16-22}$ and functionalized cobalt porphyrins $^{23-29}$ and corroles 28,30 are major classes of molecular catalysts for the two-electron transformation. In junction with a molecular photosensitizer and a sacrificial electron donor, these catalysts yield H_2 with turnover numbers (TONs) up to $\sim 10,000$ with respect to catalyst and longevities ranging from minutes to hours. An array of possible conditions including a large library of photosensitizers, sacrificial donors, and solvents makes a simple diagnosis of all systems difficult. Nevertheless, the advantages of a catalyst can still be evident when weighed against the elements it is paired with.

The ability of a proton reduction catalyst to function in water, the primary substrate, is a critical feature.^{6,9,31} Despite water being the favored solvent, many molecular hydrogen-evolution catalysts require organic solvent, with organic acids or water added to provide protons.^{6,9,10,15} One significant progression was the development of catalysts functioning in water rather than a solvent mixture.¹¹ However, the catalysts that do function in water typically require acidic conditions for optimal function (Table S1).^{6,10,11} One of the next steps for molecular catalysts is achieving high activity at neutral pH.^{9,11,18} A catalyst that functions at neutral pH is desirable because a full water-splitting system must coordinate water oxidation and aqueous proton reduction, which are thermodynamically favored at high pH and low pH, respectively (equations 2 and 3). In addition, natural water sources that are the desired solvent and substrate for photochemical water-splitting systems exist near neutral pH. A few examples of cobalt catalysts capable of photochemical proton reduction at or near neutral pH are #1, a cobalt polypyridyl catalyst that maintains TONs up to

approximately 2400, and #2, a cobalt glyoxime (see Table S1, S2 for catalysts discussed herein as well as additional examples). ^{13,18} Cobalt porphyrin catalyst #3, which achieves TONs as high as 6410, and #4 both achieve their best function near pH 7. ^{25,26}

Here, we present a metallopeptide catalyst for hydrogen evolution³² in a photochemical system that aligns well with aforementioned criteria – the easily prepared catalyst evolves hydrogen from water with no added organic solvent. Furthermore, it displays good longevity and activity near neutral pH and is activated by a photosensitizer absorbing visible light. The catalyst is a cobalt tripeptide (Gly-Gly-His, or GGH) complex (CoGGH).³² The GGH tripeptide is a model of the ATCUN (amino-terminal copper- and nickel-binding) motif found at the N-terminus of some proteins and bioactive peptides.33,34 This XXH motif coordinates metals through the Nterminal amine, the amide nitrogens of residues 2 and 3 (here, G and H), and the His imidazole No (Figure 1). As an electrocatalyst, CoGGH forms H₂ from water at an overpotential of ~600 mV (determined using the half-wave potential) with a TON of 275 at pH 8.0.32 In this report, we show that pairing CoGGH with tris(bipyridine)ruthenium(II) chloride (Ru²⁺) as a photosensitizer and ascorbate as a sacrificial electron donor near neutral pH, using either green (530 nm) or blue (447.5 nm) irradiation, system lifetimes over 100 hours and TONs up to 2200 are achieved, depending on conditions. We also show that the system performance in terms of longevity and TON is primarily limited by the photosensitizer rather than the catalyst. In summary, CoGGH is notable for being an easily synthesized metallopeptide complex for catalyzing hydrogen evolution in a visible lightdriven photochemical system in water near neutral pH.

Figure 1. Cobalt Gly-Gly-His (CoGGH)

Materials and Methods

Materials: L-ascorbic acid (Fisher Scientific), triethanolamine (Sigma Aldrich), Gly-Gly-His (Sigma Aldrich), and [Ru(bpy)₃]Cl₂ (Sigma Aldrich) were used without further purification.

CoGGH preparation and purification: Co(III)GGH was prepared, purified, and characterized according to reported procedures.³²

Hydrogen evolution studies: Fresh stock solutions of 0.5 M ascorbic acid, of 5.0 mM [Ru(bpy)₃]Cl₂, and of 500 μM CoGGH were prepared in 1.0 M MOPS buffer (pH 7.1) in doubly deionized water. The components were diluted to desired concentrations in 1.0 M MOPS (pH 7.1) to yield 5.0-mL solutions. Solution pH was adjusted to 7.1 using small amounts of NaOH when needed. Samples at pH 6.5 or 8.5 were prepared in a similar manner, with stock solutions prepared at the desired pH and solution pH adjusted with HCl or NaOH. Absorption spectra of samples were collected on a Shimadzu 8452 UV-vis absorption spectrometer before and after experiments. Most experiments used ascorbate as the sacrificial electron donor. When triethanolamine (TEOA) was used as an electron donor, stock solutions of 0.5 M TEOA, of 5.0 mM [Ru(bpy)₃]Cl₂, and of 500 uM CoGGH were prepared in 1.0 M MOPS buffer at pH 8.1 and diluted into 1.0 MOPS buffer pH 8.1. During experiments, each 5-mL solution was placed into a 41-mL vial, leaving a headspace of approximately 36-mL, and sealed with a gas-tight cap and a septum and placed in a temperaturecontrolled block connected to a Thermotek circulating water bath at 15 °C. Green (530-nm) or blue (447.5-nm) light-emitting diodes (Philips LumiLED Luxeon Star Hex 700 mA LEDS mounted on a 20-mm Star-shaped CoolBases) irradiated the vials from below. This assembly was mounted on a Thermo-Scientific MaxQ orbital shaker and the solutions were mixed by orbital shaking at 100 revolutions per minute. Before each experiment, the samples were degassed for 30 minutes by purging with a mixture of 79.31%/20.69% N₂/CH₄ (Airgas) as a reference for product quantification. At the beginning of each experiment, the power of each LED was set to 0.15 W, as measured with a L30A thermal sensor and Nova II power meter (Ophir-Spiricon LLC) placed over each LED. The light power was measured again at the end of each experiment and no significant changes were observed. Each 5-mL solution prepared for irradiation has a path length of 1.2 cm. The pH of each solution at the end of the experiment was measured, and no change larger than 0.1 pH units was observed.

To monitor H_2 evolution, 25 μ L of headspace gas was withdrawn from each vial through a septum with a gas-tight syringe (Hamilton) at defined time intervals. Headspace gas samples were analyzed on a Shimadzu GC-2014 gas chromatograph (GC) with a thermal conductivity detector and a 5-Å molecular sieve column (30 m \times 0.53 mm) to quantify the H_2 evolved. For quantification, a standard curve was prepared by injecting known volumes of H_2 into a vial containing CH_4 (from the purging gas mixture) as the internal standard. GC measurements of the corresponding known volumes are used to prepare a standard calibration curve of the ratio of H_2/CH_4 vs volume of H_2 (in mL). The GC injection temperature was 130 °C, the N_2 gas pressure was set to 34.2 PSI, the column temperature was 30 °C and the detector temperature was 130 °C.

Luminescence quenching: Steady-state emission quenching of photoexcited $[Ru(bpy)_3]^{2+*}$ (* $\mathbf{Ru^{2+}}$) (500 μ M $[Ru(bpy)_3]^{2+}$ in solution) by ascorbic acid (0-25 mM) or Co(III)GGH (0-10 μ M) in a solution under nitrogen was measured using a fluorometer (Acton Research). $[Ru(bpy)_3]^{2+}$ ($\mathbf{Ru^{2+}}$) was excited at 460 nm and emission was monitored between 530-800 nm with a slit width of 1.5 mm and integration time of 500 ms. The observed quenching behavior was fit to the Stern-Volmer equation: $I_0/I = K_{SV}[Q] + 1$ where I_0 and I describe the maximum luminescence intensity in the absence and presence of quencher, respectively, [Q] is the concentration of the quencher and K_{SV} is the Stern-Volmer constant. Quenching rate constants (k_q) were calculated by using the triplet state decay lifetime (τ_0) of 620 ns for * $\mathbf{Ru^{2+}}$ in water and fitting to the equation $K_{SV} = k_q \tau_0$. 35

Results and Discussion

Initiation of Catalysis

Catalysis utilizes three components: a sacrificial electron source, photosensitizer, and catalyst for proton reduction. The choice of archetypal $\mathbf{Ru^{2+}}$ as the photosensitizer allows for broad comparisons to other molecular systems. Ascorbic acid serves in the three-component system as a sacrificial electron source, with monoprotonated ascorbate expected to act as the primary donor species. The catalyst exists as $\mathbf{Co(III)GGH}$ prior to initiation of catalysis (Figure S1). All three components are required for appreciable hydrogen generation after visible green (530 nm) or blue (447.5 nm) light excitation of $\mathbf{Ru^{2+}}$ (Figure S2).

Reductive quenching and oxidative quenching are the two primary electron transfer quenching pathways for *Ru²⁺. In the reductive quenching pathway, photoexcited *Ru²⁺ is reduced by the sacrificial electron donor to form Ru+, which reduces the catalyst. In an oxidative quenching pathway, *Ru²⁺ is oxidized by the catalyst, forming reduced catalyst and Ru³⁺. The sacrificial electron donor then regenerates Ru²⁺ by reducing Ru³⁺.41,42 To help elucidate which quenching pathway is at work in our system, the luminescence quenching of *Ru²⁺ by both ascorbate and Co(III)GGH was investigated. A plot of I_0/I , where I and I_0 are the maximum emission intensity of *Ru²⁺ with and without quencher, respectively, was prepared as a function of ascorbate concentration (Figure S3) or Co(III)GGH concentration (Figure S4). Stern-Volmer analysis yields a bimolecular rate constant (k_0) of 3.4 x 10⁷ M⁻¹s⁻¹ for quenching by ascorbate, which is in broad agreement with literature values. 18,19,25,43 Quenching by Co(III)GGH is significantly more efficient, with a k_a of 2.8 x 10^{10} M⁻¹s⁻¹. Under optimized conditions in experiments here, the ascorbate concentration (0.1 M) is 10⁴ times greater than CoGGH concentration (10 µM), resulting in effective rates for quenching *Ru²⁺ by ascorbate and CoGGH of 3.4 x 10⁶ s⁻¹ and 2.8 x 10⁵ s⁻¹, respectively. Thus, ascorbate is expected to be the primary *Ru²⁺ quencher under experimental conditions that yield H₂, resulting in a reductive quenching pathway dominating for H₂ production (Figure S5).

The appearance of the UV-visible absorption spectrum of a reaction mixture containing 0.1 M ascorbate, 10 μ M Ru^{2+} , and 1.5 mM CoGGH, before and after irradiation indicates that the Co(III)GGH catalyst is reduced while hydrogen is produced, marked by the reduction in intensity of the ligand-field bands at 536 nm and 447.5 nm characteristic of the Co(III) species (Figure S6). In addition, the catalytic feature for hydrogen production observed by cyclic voltammetry (-1.0 V vs NHE) is proposed to be related to the Co(II/I)GGH potential.³² This potential indicates an endergonic process for direct reduction by * Ru^{2+} ($Ru^{3+}/*Ru^{2+}$ E° = -0.84V), ^{42,44} further implicating a reductive quenching pathway.

As noted, we observe a high quenching rate constant of 2.8 x 10¹⁰ M⁻¹s⁻¹ from Stern-Volmer analysis of *Ru²⁺ quenching by Co(III)GGH. Stern-Volmer behavior is assessed under steady-state conditions that do not distinguish between electron transfer and energy transfer.⁴⁵ Notably, energy transfer is possible because there is overlap between the *Ru²⁺ emission and the Co(III)GGH absorbance spectra (Figure S7). Energy transfer from *Ru²⁺ to low-lying cobalt *d-d*

states, seen elsewhere, is a probable reason for the efficient quenching. 19,21,46 While it would be pertinent to perform the same studies on Co(II)GGH, spectral overlap will still complicate steadystate analysis (Figure S7), and the catalyst is not reduced to Co(II)GGH by ascorbate in solution (Figure S1).⁴⁷ The $k_{\rm q}$ observed here with Co(III)GGH is a similar order of magnitude as the rate constants for quenching of *Ru²⁺ by cobalt catalysts #6, ²⁶ #3, ⁴⁸ and #7. ²¹

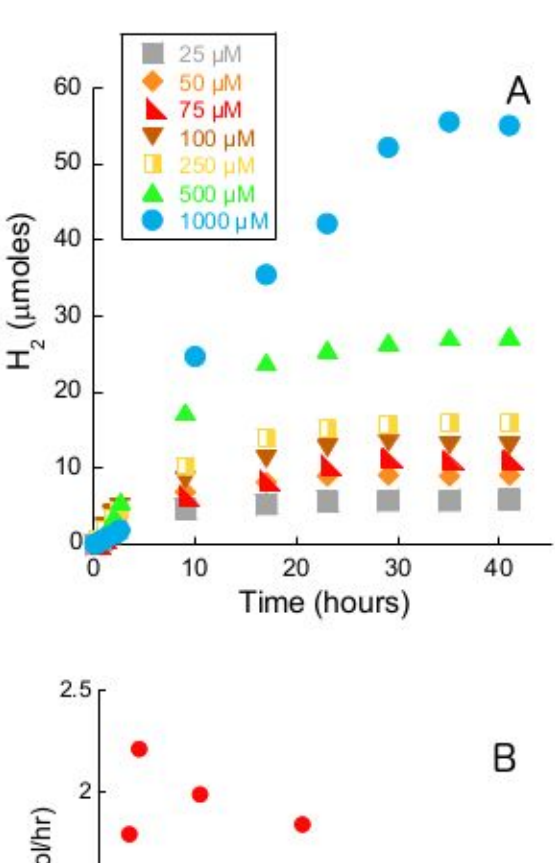
The conclusion that reductive quenching dominates is the interpretation largely made across systems using Ru²⁺ and ascorbate. Most cobalt catalysts possess a Co(II/I) reduction potential that is too negative to favorably accept an electron from *Ru2+.10,18,19,21,26 Reactions capable of proceeding by an oxidative quenching pathway feature cobalt catalysts with thermodynamically accessible potentials, but even in these examples, the overwhelming concentrations of sacrificial donor tend to favor reductive quenching. 14,19,49 Varying the sacrificial electron source can also influence the quenching pathway. In water, it has been shown that TEOA is unable to reductively quench $*Ru^{2+}$ to form Ru^+ , but can regenerate Ru^{2+} from Ru^{3+} . 50,51 Thus, reactions were designed containing 0.1 M TEOA (pK_a = 7.8), 100 μ M Ru²⁺ and 10 μ M CoGGH at pH 8.1 (note that amine donors are active when pH > pKa, and CoGGH is active for electrocatalytic³² and photochemical H₂ production in this pH range, Figure S8). Upon irradiation, no H₂ was detected (Figure S9). The same observation was made in an attempt to promote oxidative quenching in a photochemical H₂ production reaction utilizing Ru²⁺ with TEOA.⁵² However, it should be noted there is a delicate balance of factors that can contribute to performance across different pH values.38

Effect of Photosensitizer Concentration on H2 Production

The dependence of H₂ production on photosensitizer concentration was probed by varying the concentration of Ru^{2+} (0 – 1000 μ M) while keeping the concentrations of CoGGH (5 μ M) and ascorbate (0.1 M) constant. The amount of H₂ was monitored using blue irradiation at approximately 20-minute intervals for the first three hours of catalysis and then at six-hour intervals over 40 hours (Figure 2). Under these conditions, as $[\mathbf{Ru^{2+}}]$ is increased up to a value of 1000 μM, the total amount of H₂ produced increases (up to 55.6 μmol H₂, Figure S10). The initial rates of H₂ production (Figure 2B) were estimated using data obtained within the first three hours of each reaction (Figure S11). The initial rate increases linearly with Ru²⁺ concentrations up to

 μ M (to 2.2 μ mol/hr), and then decreases (to 0.73 μ mol/hr) as [Ru^{2+}] is raised further (Figure 2B).

Parallel experiments were conducted using green light for excitation, and similar general trends are observed (Figure S12). The system shows greater longevity with green light excitation, and the amount of H_2 evolved was monitored at approximately 30-minute intervals over the first five hours and then at six-hour intervals over 110 hours. The amount of hydrogen evolved increases (to 16.5 µmol H_2 , Figure S13) as the concentration of $\mathbf{Ru^{2+}}$ is increased to 100 µM. Further increasing the [$\mathbf{Ru^{2+}}$] to 1000 µM causes a decrease in total hydrogen evolved (to 6.5 µmol H_2), differing from the trend observed with blue light. The initial rates of hydrogen production are estimated from data collected in the first five hours of catalysis (Figure S14). The initial rates of hydrogen production are linear with $\mathbf{Ru^{2+}}$ concentrations up to 100 µM (to 0.23 µmol/hr) then decrease (to 0.033 µmol/hr) as [$\mathbf{Ru^{2+}}$] is raised further (Figure S12). A summary of results obtained using green and blue irradiation is shown in Table S3.



Be (hmol/hr) 1.5
0.5
0 200 400 600 800 1000
Ru²⁺ Concentration (µM)

Figure 2. (A) Effect of $[Ru(bpy)_3]^{2+}$ concentration (0, 25, 50, 75, 100, 250, 500, 1000 μ M) on H₂ production with 5 μ M CoGGH and 0.1 M ascorbate in 1.0 M MOPS, pH 7.1 with blue (447.5 nm) irradiation. (B) Initial rates for data in (A).

Using the higher energy blue light provides a ~10-fold increase in the maximum initial rate observed compared to green light (2.2 μ mol/hr versus 0.23 μ mol/hr). This effect may be attributed to more effective excitation of Ru^{2+} , which has a λ_{max} in the visible region corresponding more closely with the blue LED wavelength. With both green and blue irradiation, increases are observed in initial rates as $[Ru^{2+}]$ is increased to 100 μ M. As $[Ru^{2+}]$ is raised further, there is a steep decrease in initial rates. An increase in H_2 production rate and/or yield with increasing

photosensitizer concentration is seen in related studies. 16,18,26,48,51,53,54 In some cases, continuing to increase the concentration of photosensitizer slightly diminishes^{30,55} or causes a plateau in the total amount of hydrogen produced. 16-18,26,51 The sharp decrease in initial rate observed here as photosensitizer concentration is increased is less common. As noted elsewhere, there is a delicate balance in achieving an optimal ratio of sensitizer to catalyst, and unproductive electron transfer processes may be fueled by high concentrations of photosensitizer relative to catalyst.⁵⁶ With other factors remaining constant, as photosensitizer concentration increases there will be more *Ru²⁺ available to be reduced by ascorbate to \mathbf{Ru}^+ , which supplies electrons to the catalyst. At low $[\mathbf{Ru}^{2+}]$ (≤ 100 μM here), the amount of light that can be absorbed and the consequent charge separation has been implicated as the process limiting catalysis. 18,51 However, at relatively high photosensitizer concentrations ($\geq 100 \mu M$), the rate of H₂ production may become limited by the scavenging of electrons from Ru⁺ by the catalyst. 16,19 In addition, the dechelation reaction associated with photosensitizer decomposition, in which a bipyridine ligand is replaced by water or ascorbate, is exacerbated by accumulation of this reactive **Ru**⁺ species. ^{16,18,19,57,58} We expect that processes associated with activity loss at high [Ru2+] are homogeneous in nature, because dynamic light scattering experiments on the reaction mixtures collected before and after catalysis with high [Ru²⁺] (500 μM) do not indicate formation of nanoparticles (Figure S15), which also may be a significant contributor to the decreases in initial rate when they are formed.

While blue light provides an increase in maximum initial rates, it is at the cost of system longevity, with activity lasting for 40 hours rather than 110 hours with green light. Decomposition of the sensitizer is evident from comparison of the absorption spectra of 100 µM Ru^{2+} , 10 µM CoGGH and 0.1 M ascorbate before and after illumination with both blue and green light (Figure S16). Using blue light results in a greater amount of change of the absorption spectrum of Ru^{2+} over the course of a typical experiment. A decrease in the intensity of the Ru^{2+} MLCT band at 460 nm is seen, similar to other cases where degradation is observed. When #11 was used in junction with Ru^{2+} and ascorbic acid to fuel hydrogen production, a broad peak at 477 nm, redshifted from the Ru^{2+} MLCT band, was attributed to a degradation product. This observation is consistent with the spectrum of Ru^{2+} observed after 40 hours of photocatalysis fueled by blue light, featuring a broad peak around 480 nm.

In the system with green light, monitoring the absorption spectrum of $\mathbf{Ru^{2+}}$ also reveals a lowered intensity of the MLCT band, along with the appearance of a broad peak around 530 nm after photocatalysis (Figure S16). Competitive light absorption by degradation products has been shown to have a detrimental effect on catalysis with # $\mathbf{10^{19}}$ and # $\mathbf{11^{18}}$ While total hydrogen evolved with blue light increases with high concentrations of [$\mathbf{Ru^{2+}}$], the same trend was not observed at high concentrations of [$\mathbf{Ru^{2+}}$] with green light. Green irradiation corresponds more directly than blue to where the degradation product absorbs. Unproductive light absorption by $\mathbf{Ru^{2+}}$ degradation products may lead to the decreases in total hydrogen production observed with green light at high [$\mathbf{Ru^{2+}}$] (Figure S10).

Effect of Catalyst Concentration on H2 Production

As with the concentration of the photosensitizer, the impact of catalyst concentration on H_2 production was evaluated. The effect of increasing the concentration of CoGGH (0 - 50 μ M) with constant concentrations of Ru^{2+} (100 μ M) and ascorbate (0.1 M) on H_2 production was monitored with blue irradiation (Figure 3). The amount of H_2 was monitored at approximately 20-minute intervals for the first three hours of catalysis (Figure S17) and then at six-hour intervals over 40 hours (Figure 3A). The amount of H_2 produced increases linearly with increasing catalyst concentration up to 10 μ M, with a more shallow increase at higher concentrations (Figure S18). Initial rates were determined from data collected over the first 3 hours of each reaction where the amount of H_2 produced as a function of time is linear. The initial rates show a linear dependence on [CoGGH], reaching a maximum (2.3 μ mol H_2 /hr) rate at 10 μ M CoGGH (Figure 3B). As [CoGGH] is increased above 10 μ M, the initial rates plateau.

The impact of varying [CoGGH] was also studied with green irradiation (Figure S19). The amount of H_2 was monitored at approximately 30-minute intervals for the first five hours (Figure S20) of catalysis and then at six-hour intervals over 110 hours. The amount of H_2 produced increases with increasing catalyst concentration, with 50 μ M CoGGH producing the largest amount of H_2 (17.9 μ mol H_2 ; Figure S21). The slopes of data from the first 5 hours of each reaction were used to estimate initial rates. Up to 10 μ M, the initial rates increase as the concentration of CoGGH is increased (Figure S19). A full summary of results with blue and green light is shown in Table S3.

With both blue and green irradiation, the amount of hydrogen produced increases with increasing catalyst concentration. Similar total H_2 amounts are achieved with both blue and green light (20 µmol H_2 and 17.9 µmol H_2 , respectively). Comparable concentration dependent increases are observed with other cobalt catalysts, often with total production and rates plateauing around a similar catalyst concentration. 18,26,48,55,59,60 With both wavelengths, the initial rates display a linear dependence on catalyst concentration at low value (up to ~ 10 µM CoGGH), providing some evidence that the reaction is homogeneous at low catalyst concentrations. An assumption of homogeneity warrants some wariness since cobalt nanoparticles may account for the activity of some water reduction and oxidation catalysts. 16 Although dynamic light scattering experiments before and after catalysis do not indicate nanoparticle formation (Figure S15), mercury poisoning tests were performed to further confirm the absence of nanoparticle formation impacting catalysis (Figure S22).

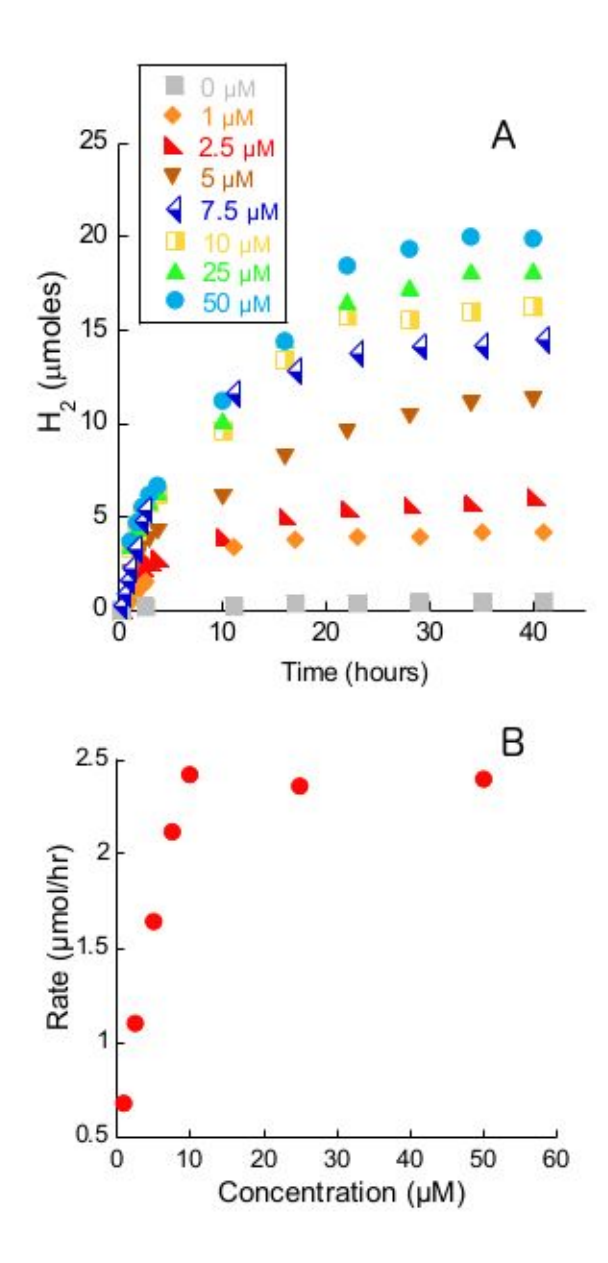


Figure 3. (A) Effect of CoGGH concentration $(0, 1, 2.5, 5, 7.5, 10, 25, 50 \,\mu\text{M})$ on H₂ production with 100 μ M [Ru(bpy)₃]²⁺ and 0.1 M ascorbate in 1.0 M MOPS, pH 7.1 with irradiation with blue (447.5-nm) light. (B) Initial rates for data in (A).

Since there are many possible pathways to hydrogen evolution (and many competing side reactions), discerning mechanistic steps in photochemical systems is challenging. Commonly invoked possibilities for photocatalytic hydrogen evolution from cobalt catalysts are shown in Figure S23. A major distinction is between heterolytic and homolytic pathways, referring to the type of Co-H bond cleavage. A first-order dependence of initial rate on cobalt concentration

suggests a heterolytic, single-cobalt mechanism. This is a common observation and conclusion for cobalt catalysts at low concentration and under similar conditions to those here, with examples including #6,²⁶ #10,¹⁹ #12,⁶⁰ and #13.¹⁷ A less common observation, made for #14 paired with a rhenium sensitizer, is that the initial rate for H₂ production is linearly dependent on the square of the concentration of the catalyst, which implies a two-cobalt, homolytic pathway.⁶¹ Here, the initial rates show a first-order dependence on catalyst concentrations up to ~10 μM (Figure 3B, Figure S19), supporting the proposal that a single-site, heterolytic mechanism is active under those conditions. While electrochemical data indicate that reduction of Co(II) to Co(I) is involved in catalysis³² and UV-vis data support a reduction from Co(III)GGH (Figure S6), confirming photochemical mechanistic steps under relevant conditions requires further study. Promising transient absorption and spectroelectrochemistry experiments have revealed reaction kinetics and implicated Co(I) species for catalysis by #15,⁶² #11,¹⁸ and #4,²⁵ and efforts to employ these techniques to discern the mechanism are ongoing.

Table 1. A summary of selected results from this work alongside relevant examples operative near neutral pH.

Catalyst	[Catalyst] (µM)	[Ru ²⁺] (µM)	Time (hr)	TON _{Co}	Wavelength (nm)	pН	ref.
CoGGH	5	1000	35	2200	447.5	7.1	a
	10	100	35	325	447.5	7.1	a
	1	100	35	860	447.5	7.1	a
	1	100	110	980	530	7.1	a
#1	1.25	330	14^b	2400^{b}	452	7	18
#2	0.2	N/A ^c	2	73	>420	7	13
#3	1.5	1200	1	6410	420	6.8	26
#4	2.5	1000	4	725	>400	7	25

^aThis work; ^bEstimated from figure; ^cEosin Y is utilized as sensitizer

Turnover Numbers and Longevity

The analysis of visible light driven hydrogen production with CoGGH yielded promising results: TONs up to 2200 were facilitated by blue light irradiation over 40 hours, and green light irradiation sustained catalysis for over 100 hours to yield nearly 1000 turnovers. The sensitivity of turnover numbers to changing conditions can make direct literature comparisons complicated. Nevertheless, comparison to closely related systems shows that the TONs achieved with CoGGH are promising. As noted, high TONs achieved by the majority of reported cobalt catalysts are at acidic pH (Table S1). The TONs observed here are competitive with some of these cobalt catalysts paired with **Ru**²⁺ as a photosensitizer, such as #10,¹⁹ #11,¹⁸ #16,¹⁴ and #7.²¹ Importantly, though, CoGGH shows activity for hydrogen production between pH 6.5 and pH 8.5, with optimal performance achieved near neutral pH (Figure S8). This is outside of the range where most cobalt catalysts achieve optimal function. Examples of cobalt catalysts functioning near neutral pH are highlighted alongside data collected with CoGGH in Table 1.

As observed with many cobalt polypyridyl catalysts, for CoGGH there is a significant increase in TON as catalyst concentration is lowered (Figure 4A). 17,18,54,57 Occasionally, reported TONs are relatively insensitive to catalyst concentration. While this is sometimes attributed to experimental conditions like light intensity, 19 it has also been linked to the catalyst limiting the performance of the system. 46,51,63 In the case of cobaloxime catalysts, this behavior has been attributed to catalyst degradation, requiring replenishment of the dimethylglyoxime ligand to improve TONs. 12,46,59,61,64

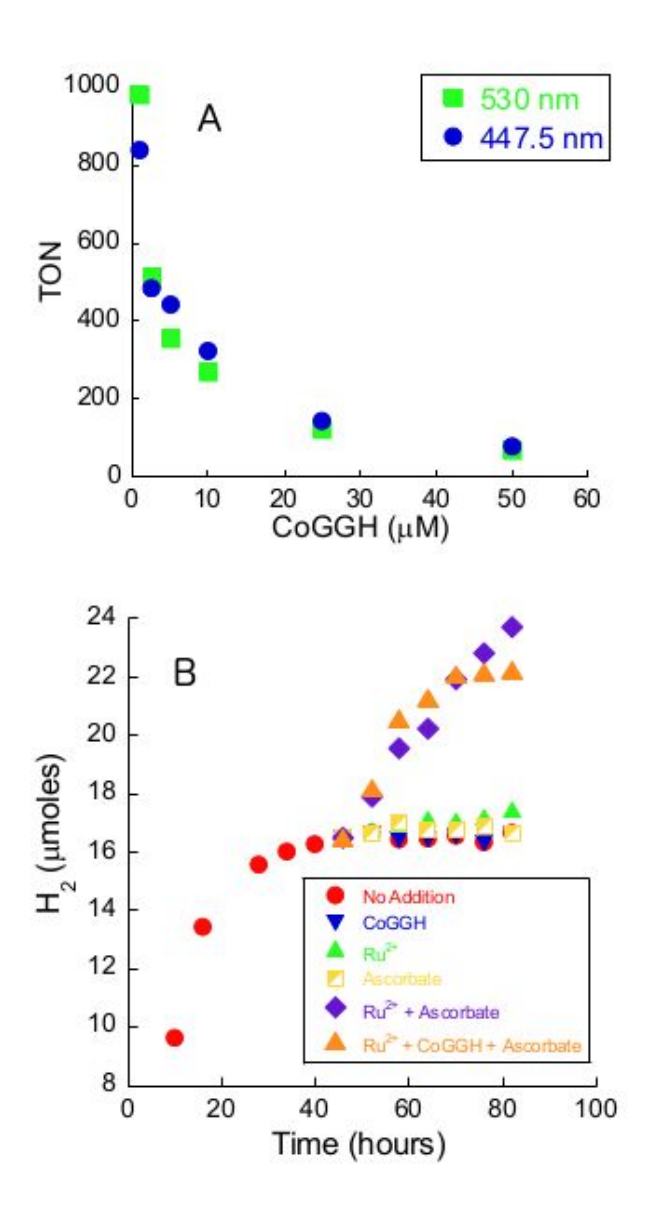


Figure 4. (A) Effect of CoGGH concentration (1, 2.5, 5, 10, 25, 50 μM) on TON for H₂ production with 100 μM [Ru(bpy)₃]²⁺ and 0.1 M ascorbate at in 1 M MOPS, pH 7.1. TON is evaluated where activity plateaus, for green irradiation at 110 hours and for blue irradiation at 35 hours. **(B)** H₂ produced from 100 μM [Ru(bpy)₃]²⁺ and 10 μM CoGGH in presence of ascorbate (0.1 M) as the electron donor, with fresh addition of 10 μM CoGGH, 100 μM [Ru(bpy)₃]²⁺ and/or 0.1 M ascorbate after 40 hours (447.5 nm irradiation). The particular components replenished are: none (red circles), 10 μM CoGGH, 100 μM [Ru(bpy)₃]²⁺ and 0.1 M ascorbate (orange triangles), 100 μM [Ru(bpy)₃]²⁺ and 0.1 M ascorbate (purple diamonds), 100 μM [Ru(bpy)₃]²⁺ (green triangle), 0.1 M ascorbate (yellow square), 10 μM CoGGH (blue triangle). Data for green irradiation are shown in Figure S24.

Among other useful general benchmarks for comparison is longevity. While blue light fostered the highest TONs, catalysis fully plateaus by 35 hours. On the other hand, green light extends the lifetime of catalysis over 100 hours, but the slower H_2 production rate yields modestly lower TONs. As discussed above, the degradation of $\mathbf{Ru^{2+}}$ is a known problem, and is exacerbated by the use of blue light (Figure S16). Even so, system lifetimes here are favorable compared to most other cobalt catalysts paired with $\mathbf{Ru^{2+}}$, typically lasting from minutes to less than a day. 10,16-21,25,46 This observation suggests that CoGGH may be quite stable under the conditions used.

In some systems, catalyst degradation impacts performance alongside sensitizer degradation. To determine the components limiting the lifetime of catalysis in this system, the reaction consisting of 100 μ M Ru^{2+} , 0.1 M ascorbate and 10 μ M CoGGH was replenished with fresh photosensitizer, electron donor, and/or catalyst after activity began to plateau. After 40 hours of irradiation with blue light, additions were made and H_2 production was monitored for another 40 hours (Figure 4B). Addition of each individual component (0.1 M ascorbic acid, 100 μ M Ru^{2+} , or 10 μ M CoGGH) regenerated 1.9%, 6.2%, or 0.8% of activity, respectively. However, replenishing both Ru^{2+} (100 μ M) and ascorbic acid (0.1 M) regenerated 44% of activity. The fresh addition of all three components regenerates nearly the same amount of activity as replenishing only Ru^{2+} and ascorbic acid, 37%.

Parallel experiments using green light have greater longevity, but reflect the same trends observed with blue (Figure S24). A reaction mixture consisting of 100 μ M Ru^{2+} , 0.1 M ascorbate and 10 μ M CoGGH was replenished with fresh photosensitizer, electron donor, and/or catalyst as activity began to slow after 48 hours. Hydrogen production was monitored over another 110 hours after replenishment. Addition of each individual component (0.1 M ascorbic acid, 100 μ M Ru^{2+} , or 10 μ M CoGGH) recovered 1.7%, 2.7%, or 9.3% of activity, respectively. Replenishing both Ru^{2+} (100 μ M) and ascorbic acid (0.1 M) regenerated 31% of activity, and the addition of all three components regenerated 34%.

Although the lifetime of catalysis is different, the total percentages of activity regenerated using either green or blue light are similar. Replenishing single components (0.1 M ascorbic acid, $100 \, \mu M \, Ru^{2+}$, or $10 \, \mu M \, CoGGH$) regenerates little activity. Although the addition of fresh Ru^{2+} regenerates the most activity among the single component additions in both cases, still less than 10% is recovered. Ascorbate is present in significant excess relative to the other components, and

it has been shown elsewhere that an excess remains throughout photocatalysis. ¹⁹ Paired with the lack of activity recovered by addition of ascorbate, it is unlikely that the availability of the sacrificial electron donor is a limiting factor. Addition of CoGGH does not significantly rescue the activity of our system, indicating that catalyst decomposition is not a limiting factor. The absorbance spectrum of CoGGH shows only slight changes when irradiated across the time frame of catalysis with green light, indicating it is not suffering from direct photodegradation (Figure S25). Changes in the spectrum of CoGGH are more evident after irradiation with blue light (Figure S26), making it surprising that CoGGH replenishment fails to enhance activity.

To regenerate appreciable activity, it is necessary to add multiple components. Replenishing both ascorbic acid and Ru²⁺ or all three components recovers nearly the same amount of activity (between 30-40%). Although it seems that decomposition of Ru²⁺ is the primary limiting factor in catalysis, minimal activity regeneration upon adding Ru²⁺ alone is likely related to the accumulation of side products, foremost dehydroascorbic acid (DHA), 19,38,48,65,66 which is formed from disproportionation of the ascorbate radical anion produced by reducing *Ru²⁺.62 Time-resolved studies on the interaction of Ru²⁺ with ascorbate and its oxidation products have shown evidence of back electron transfer from *Ru2+ to both the oxidized ascorbate anion and DHA.66 As DHA becomes more concentrated throughout the course of the experiment, electron transfer to DHA becomes competitive with productive electron transfer, slowing or stopping catalysis. 17,65,66 This effect was demonstrated with deliberate addition of dehydroascorbic acid to the photochemical assembly containing #10, reducing the amount of H₂ generated. ¹⁹ Regenerating both ascorbic acid and Ru²⁺ in our experiments should restore productive electron transfer.⁶⁵ However, DHA is not removed after accumulating over the course of the experiment, which may prevent 100% activity recovery.65 Reduction of DHA by a terminal electron donor, tris(2carboxyethyl)phosphine (TCEP), has recently been reported to lead to large improvements in activity and may be a viable strategy to renew full activity in future work. ^{22,67} Given the evidence that CoGGH is relatively stable in these experiments, it is expected that substituting Ru²⁺ with a more robust photosensitizer such as a quantum dot will yield both a longer lasting system and higher TONs.68,69

Conclusions

We have demonstrated that a simple cobalt metallopeptide catalyzes H₂ production from neutral water in a light-driven reaction. A TON of 2200 with respect to CoGGH was observed when blue light is used for excitation, and the catalyst shows exceptional longevity. Early diagnosis of CoGGH in a light-driven photocatalytic system has allowed for proposals of mechanisms centered at **Ru**. Future work will consist of mechanistic studies of the photocatalytic process, the use of metallopeptide catalyst derivatives, and the employment of more robust photosensitizers.

Acknowledgements: The authors thank the National Science Foundation grant CHE-1708256 for support of this work. E. H. E. acknowledges support from T32-GM118283.

Supporting Information: Additional experimental results and tabulated data including UV-vis spectra, Stern-Volmer quenching experiments, gas chromatographs, emission data, pH dependence of hydrogen evolution, dynamic light scattering experiments, results collected using green LED irradiation, tables of results on related complexes from the literature, and a table of results obtained herein.

References

- (1) Lewis, N. S.; Nocera, D. G. Powering the Planet: Chemical Challenges in Solar Energy Utilization. *Proc. Natl. Acad. Sci. U.S.A.* **2006**, *103*, 15729-15735.
- (2) Han, Z.; Eisenberg, R. Fuel from Water: The Photochemical Generation of Hydrogen from Water. *Acc. Chem. Res.* **2014**, *47*, 2537-2544.
- (3) Gray, H. B. Powering the Planet with Solar Fuel. *Nat. Chem.* **2009**, *1*, 7.
- (4) McKone, J. R.; Lewis, N. S.; Gray, H. B. Will Solar-Driven Water-Splitting Devices See the Light of Day? *Chem. Mater.* **2014**, *26*, 407-414.
- (5) Gust, D.; Moore, T. A.; Moore, A. L. Solar Fuels Via Artificial Photosynthesis. *Acc. Chem. Res.* **2009**, *42*, 1890-1898.
- (6) Artero, V.; Chavarot-Kerlidou, M.; Fontecave, M. Splitting Water with Cobalt. *Angew. Chem. Int. Ed.* **2011**, *50*, 7238-7266.
- (7) Bren, K. L. Multidisciplinary Approaches to Solar Hydrogen. J. R. Soc. Interface 2015, 20140091.

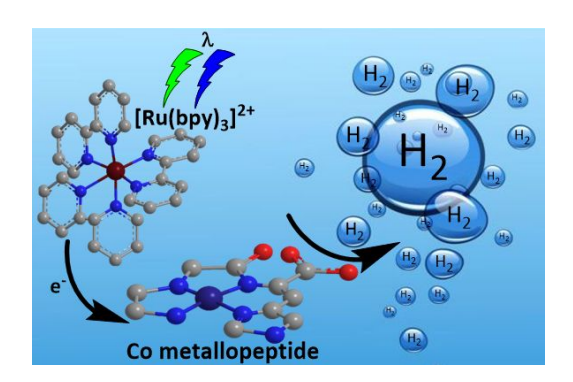
- (8) Anastas, P.; Eghbali, N. Green Chemistry: Principles and Practice. *Chem. Soc. Rev.* **2010**, *39*, 301-312.
- (9) Du, P.; Eisenberg, R. Catalysts Made of Earth-Abundant Elements (Co, Ni, Fe) for Water Splitting: Recent Progress and Future Challenges. *Energy Environ. Sci.* **2012**, *5*, 6012-6021.
- (10) Queyriaux, N.; Jane, R. T.; Massin, J.; Artero, V.; Chavarot-Kerlidou, M. Recent Developments in Hydrogen Evolving Molecular Cobalt(II)-Polypyridyl Catalysts. *Coord. Chem. Rev.* **2015**, *304*, 3-19.
- (11) Zee, D. Z.; Chantarojsiri, T.; Long, J. R.; Chang, C. J. Metal-Polypyridyl Catalysts for Electro- and Photochemical Reduction of Water to Hydrogen. *Acc. Chem. Res.* **2015**, *48*, 2027-2036.
- (12) Eckenhoff, W. T.; McNamara, W. R.; Du, P.; Eisenberg, R. Cobalt Complexes as Artificial Hydrogenases for the Reductive Side of Water Splitting. *Biochim. Biophys. Acta* **2013**, *1827*, 958-973.
- (13) Lakadamyali, F.; Kato, M.; Muresan, N. M.; Reisner, E. Selective Reduction of Aqueous Protons to Hydrogen with a Synthetic Cobaloxime Catalyst in the Presence of Atmospheric Oxygen. *Angew. Chem. Int. Ed.* **2012**, *51*, 9381-9384.
- (14) Varma, S.; Castillo, C. E.; Stoll, T.; Fortage, J.; Blackman, A. G.; Molton, F.; Deronzier, A.; Collomb, M.-N. Efficient Photocatalytic Hydrogen Production in Water Using a Cobalt(III) Tetraaza-Macrocyclic Catalyst: Electrochemical Generation of the Low-Valent Co(I) Species and Its Reactivity toward Proton Reduction. *Phys. Chem. Chem. Phys.* **2013**, *15*, 17544-17552.
- (15) Dempsey, J. L.; Brunschwig, B. S.; Winkler, J. R.; Gray, H. B. Hydrogen Evolution Catalyzed by Cobaloximes. *Acc. Chem. Res.* **2009**, *42*, 1995-2004.
- (16) Sun, Y.; Sun, J.; Long, J. R.; Yang, P.; Chang, C. J. Photocatalytic Generation of Hydrogen from Water Using a Cobalt Pentapyridine Complex in Combination with Molecular and Semiconductor Nanowire Photosensitizers. *Chem. Sci.* **2013**, *4*, 118-124.
- (17) Guttentag, M.; Rodenberg, A.; Bachmann, C.; Senn, A.; Hamm, P.; Alberto, R. A Highly Stable Polypyridyl-Based Cobalt Catalyst for Homo- and Heterogeneous Photocatalytic Water Reduction. *Dalton Trans.* **2013**, *42*, 334-337.
- (18) Khnayzer, R. S.; Thoi, V. S.; Nippe, M.; King, A. E.; Jurss, J. W.; El Roz, K. A.; Long, J. R.; Chang, C. J.; Castellano, F. N. Towards a Comprehensive Understanding of Visible-Light Photogeneration of Hydrogen from Water Using Cobalt(II) Polypyridyl Catalysts. *Energy Environ. Sci.* **2014**, *7*, 1477.
- (19) Deponti, E.; Luisa, A.; Natali, M.; Iengo, E.; Scandola, F. Photoinduced Hydrogen Evolution by a Pentapyridine Cobalt Complex: Elucidating Some Mechanistic Aspects. *Dalton Trans.* **2014**, *43*, 16345-16353.
- (20) Jurss, J. W.; Khnayzer, R. S.; Panetier, J. A.; El Roz, K. A.; Nichols, E. M.; Head-Gordon, M.; Long, J. R.; Castellano, F. N.; Chang, C. J. Bioinspired Design of Redox-Active Ligands for Multielectron Catalysis: Effects of Positioning Pyrazine Reservoirs on Cobalt for Electro- and Photocatalytic Generation of Hydrogen from Water. *Chem. Sci.* **2015**, *6*, 4954-4972.
- (21) Natali, M.; Badetti, E.; Deponti, E.; Gamberoni, M.; Scaramuzzo, F. A.; Sartorel, A.; Zonta, C. Photoinduced Hydrogen Evolution with New Tetradentate Cobalt(II) Complexes Based on the Tpma Ligand. *Dalton Trans.* **2016**, *45*, 14764-14773.
- (22) Kohler, L.; Niklas, J.; Johnson, R. C.; Zeller, M.; Poluektov, O. G.; Mulfort, K. L. Molecular Cobalt Catalysts for H2 Generation with Redox Activity and Proton Relays in the Second Coordination Sphere. *Inorg. Chem.* **2019**, *58*, 1697-1709.

- (23) Mase, K.; Aoi, S.; Ohkubo, K.; Fukuzumi, S. Catalytic Reduction of Proton, Oxygen and Carbon Dioxide with Cobalt Macrocyclic Complexes. *J. Porphyrins Phthalocyanines* **2016**, *20*, 935-949.
- (24) Ladomenou, K.; Natali, M.; Iengo, E.; Charalampidis, G.; Scandola, F.; Coutsolelos, A. G. Photochemical Hydrogen Generation with Porphyrin-Based Systems. *Coord. Chem. Rev.* **2015**, *304*, 38-54.
- (25) Natali, M.; Luisa, A.; lengo, E.; Scandola, F. Efficient Photocatalytic Hydrogen Generation from Water by a Cationic Cobalt(II) Porphyrin. *Chem. Comm.* **2014**, *50*, 1842-1844.
- (26) Beyene, B. B.; Hung, C. H. Photocatalytic Hydrogen Evolution from Neutral Aqueous Solution by a Water-Soluble Cobalt(II) Porphyrin. *Sustainable Energy & Fuels*, **2018**, *2*, 2036-2043.
- (27) Morales Vasquez, M. A.; Hamer, M.; Neuman, N. I.; Tesio, A. Y.; Hunt, A.; Bogo, H.; Calvo, E. J.; Doctorovich, F. Iron and Cobalt Corroles in Solution and on Carbon Nanotubes as Molecular Photocatalysts for Hydrogen Production by Water Reduction. *ChemCatChem* **2017**, *9*, 3259-3268.
- (28) Zhang, W.; Lai, W.; Cao, R. Energy-Related Small Molecule Activation Reactions: Oxygen Reduction and Hydrogen and Oxygen Evolution Reactions Catalyzed by Porphyrin- and Corrole-Based Systems. *Chem. Rev.* **2017**, *117*, 3717-3797.
- (29) Kleingardner, J. G.; Kandemir, B.; Bren, K. L. Hydrogen Evolution from Neutral Water under Aerobic Conditions Catalyzed by Cobalt Microperoxidase-11. *J. Am. Chem. Soc.* **2014**, *136*, 4-7.
- (30) Yuan, H.-Q.; Wang, H.-H.; Kandhadi, J.; Wang, H.; Zhan, S.-Z.; Liu, H.-Y. Electrochemical and Photocatalytic Hydrogen Evolution by an Electron-Deficient Cobalt Tris(Ethoxycarbonyl)Corrole Complex. *Appl. Organomet. Chem.* **2017**, *31*, e3773
- (31) Thoi, V. S.; Sun, Y.; Long, J. R.; Chang, C. J. Complexes of Earth-Abundant Metals for Catalytic Electrochemical Hydrogen Generation under Aqueous Conditions. *Chem. Soc. Rev.* **2013**, *42*, 2388-2400.
- (32) Kandemir, B.; Kubie, L.; Guo, Y.; Sheldon, B.; Bren, K. L. Hydrogen Evolution from Water under Aerobic Conditions Catalyzed by a Cobalt Atcun Metallopeptide. *Inorg. Chem.* **2016**, *55*, 1355-1357.
- (33) Harford, C.; Sarkar, B. Amino Terminal Cu(II)- and Ni(II)-Binding (ATCUN) Motif of Proteins and Peptides: Metal Binding, DNA Cleavage, and Other Properties. *Acc. Chem. Res.* **1997**, *30*, 123-130.
- (34) Melino, S.; Santone, C.; Di Nardo, P.; Sarkar, B. Histatins: Salivary Peptides with Copper(II) and Zinc(II)-Binding Motifs Perspectives for Biomedical Applications. *FEBS J.* **2014**, *281*, 657-672.
- (35) Kalyanasundaram, K. Photophysics, Photochemistry and Solar-Energy Conversion with Tris(Bipyridyl)Ruthenium(II) and Its Analogs. *Coord. Chem. Rev.* **1982**, *46*, 159-244.
- (36) Deponti, E.; Natali, M. Photocatalytic Hydrogen Evolution with Ruthenium Polypyridine Sensitizers: Unveiling the Key Factors to Improve Efficiencies. *Dalton Trans.* **2016**, *45*, 9136-9147.
- (37) Pellegrin, Y.; Odobel, F. Sacrificial Electron Donor Reagents for Solar Fuel Production. *C. R. Chim.* **2017**, *20*, 283-295.
- (38) Natali, M. Elucidating the Key Role of pH on Light-Driven Hydrogen Evolution by a Molecular Cobalt Catalyst. *ACS Catal.* **2017**, *7*, 1330-1339.

- (39) Brown, G. M.; Brunschwig, B. S.; Creutz, C.; Endicott, J. F.; Sutin, N. Homogeneous Catalysis of the Photoreduction of Water by Visible Light. Mediation by a Tris(2,2'-Bipyridine)Ruthenium(II)-Cobalt(II) Macrocycle System. *J. Am. Chem. Soc.* **1979**, *101*, 1298-1300.
- (40) It should be noted that with both green and blue irradiation, a small amount (\sim 0.5 µmol) of hydrogen is produced in the absence of the catalyst (Figure S2).
- (41) Arias-Rotondo, D. M.; McCusker, J. K. The Photophysics of Photoredox Catalysis: A Roadmap for Catalyst Design. *Chem. Soc. Rev.* **2016**, *45*, 5803-5820.
- (42) Bock, C. R.; Connor, J. A.; Gutierrez, A. R.; Meyer, T. J.; Whitten, D. G.; Sullivan, B. P.; Nagle, J. K. Estimation of Excited-State Redox Potentials by Electron-Transfer Quenching. Application of Electron-Transfer Theory to Excited-State Redox Processes. *J. Am. Chem. Soc.* **1979**, *101*, 4815-4824.
- (43) Krishnan, C. V.; Sutin, N. Homogeneous Catalysis of the Photoreduction of Water by Visible Light. 2. Mediation by a Tris(2,2'-Bipyridine)Ruthenium(II)-Cobalt(II) Bipyridine System. *J. Am. Chem. Soc.* **1981**, *103*, 2141-2142.
- (44) Creutz, C.; Sutin, N. Electron-Transfer Reactions of Excited States. Reductive Quenching of the Tris(2,2'-Bipyridine)Ruthenium(II) Luminescence. *Inorg. Chem.* **1976**, *15*, 496-499.
- (45) Lakowicz, J. R. Principles of Fluorescence Spectroscopy; Springer: New York, 2006.
- (46) Probst, B.; Guttentag, M.; Rodenberg, A.; Hamm, P.; Alberto, R. Photocatalytic H₂ Production from Water with Rhenium and Cobalt Complexes. *Inorg. Chem.* **2011**, *50*, 3404-3412.
- (47) Co(II)GGH Has been difficult to prepare in pure Form for Quenching Studies in the Absence of Excess Reductant (which will Interfere with the experiment by providing an additional quenching pathway) at suitable concentrations for quenching studies. Future time-dependent fluorescence and transient absorption spectroscopy will provide more detailed insight into the electron transfer steps from the excited photosensitizer.
- (48) McNamara, W. R.; Han, Z.; Alperin, P. J.; Brennessel, W. W.; Holland, P. L.; Eisenberg, R. A Cobalt-Dithiolene Complex for the Photocatalytic and Electrocatalytic Reduction of Protons. *J. Am. Chem. Soc.* **2011**, *133*, 15368-15371.
- (49) Fihri, A.; Artero, V.; Razavet, M.; Baffert, C.; Leibl, W.; Fontecave, M. Cobaloxime-Based Photocatalytic Devices for Hydrogen Production. *Angew. Chem. Int. Ed.* **2008**, *47*, 564-567.
- (50) Kalyanasundaram, K.; Kiwi, J.; Grätzel, M. Hydrogen Evolution from Water by Visible-Light, a Homogeneous 3 Component Test System for Redox Catalysis. *Helv. Chim. Acta* **1978**, *61*, 2720-2730.
- (51) Goldsmith, J. I.; Hudson, W. R.; Lowry, M. S.; Anderson, T. H.; Bernhard, S. Discovery and High-Throughput Screening of Heteroleptic Iridium Complexes for Photoinduced Hydrogen Production. *J. Am. Chem. Soc.* **2005**, *127*, 7502-7510.
- (52) Eckenhoff, W. T.; Brennessel, W. W.; Eisenberg, R. Light-Driven Hydrogen Production from Aqueous Protons Using Molybdenum Catalysts. *Inorg. Chem.* **2014**, *53*, 9860-9869.
- (53) Lazarides, T.; Delor, M.; Sazanovich, I. V.; McCormick, T. M.; Georgakaki, I.; Charalambidis, G.; Weinstein, J. A.; Coutsolelos, A. G. Photocatalytic Hydrogen Production from a Noble Metal Free System Based on a Water Soluble Porphyrin Derivative and a Cobaloxime Catalyst. *Chem. Comm.* **2014**, *50*, 521-523.
- (54) Nippe, M.; Khnayzer, R. S.; Panetier, J. A.; Zee, D. Z.; Olaiya, B. S.; Head-Gordon, M.; Chang, C. J.; Castellano, F. N.; Long, J. R. Catalytic Proton Reduction with Transition Metal Complexes of the Redox-Active Ligand Bpy₂PyMe. *Chem. Sci.* **2013**, *4*, 3934.

- (55) Luo, S. P.; Tang, L. Z.; Zhan, S. Z. A Cobalt(II) Complex of 2,2-Bipyridine, a Catalyst for Electro- and Photo-Catalytic Hydrogen Production in Purely Aqueous Media. *Inorg. Chem. Comm.* **2017**, *86*, 276-280.
- (56) Sabatini, R. P.; Lindley, B.; McCormick, T. M.; Lazarides, T.; Brennessel, W. W.; McCamant, D. W.; Eisenberg, R. Efficient Bimolecular Mechanism of Photochemical Hydrogen Production Using Halogenated Boron-Dipyrromethene (Bodipy) Dyes and a Bis(Dimethylglyoxime) Cobalt(III) Complex. *J. Phys. Chem. B* **2016**, *120*, 527-534.
- (57) Singh, W. M.; Baine, T.; Kudo, S.; Tian, S. L.; Ma, X. A. N.; Zhou, H. Y.; DeYonker, N. J.; Pham, T. C.; Bollinger, J. C.; Baker, D. L.; Yan, B.; Webster, C. E.; Zhao, X. Electrocatalytic and Photocatalytic Hydrogen Production in Aqueous Solution by a Molecular Cobalt Complex. *Angew. Chem. Int. Ed.* **2012**, *51*, 5941-5944.
- (58) Limburg, B.; Bouwman, E.; Bonnet, S. Rate and Stability of Photocatalytic Water Oxidation Using [Ru(Bpy)₃]²⁺ as Photosensitizer. *ACS Catal.* **2016**, *6*, 5273-5284.
- (59) Lazarides, T.; McCormick, T.; Du, P.; Luo, G.; Lindley, B.; Eisenberg, R. Making Hydrogen from Water Using a Homogeneous System without Noble Metals. *J. Am. Chem. Soc.* **2009**, *131*, 9192-9194.
- (60) Du, P. W.; Schneider, J.; Luo, G. G.; Brennessel, W. W.; Eisenberg, R. Visible Light-Driven Hydrogen Production from Aqueous Protons Catalyzed by Molecular Cobaloxime Catalysts. *Inorg. Chem.* **2009**, *48*, 4952-4962.
- (61) Probst, B.; Rodenberg, A.; Guttentag, M.; Hamm, P.; Alberto, R. A Highly Stable Rhenium-Cobalt System for Photocatalytic H-2 Production: Unraveling the Performance-Limiting Steps. *Inorg. Chem.* **2010**, *49*, 6453-6460.
- (62) Rodenberg, A.; Orazietti, M.; Probst, B.; Bachmann, C.; Alberto, R.; Baldridge, K. K.; Hamm, P. Mechanism of Photocatalytic Hydrogen Generation by a Polypyridyl-Based Cobalt Catalyst in Aqueous Solution. *Inorg. Chem.* **2015**, *54*, 646-657.
- (63) Zhang, P.; Wang, M.; Dong, J.; Li, X.; Wang, F.; Wu, L.; Sun, L. Photocatalytic Hydrogen Production from Water by Noble-Metal-Free Molecular Catalyst Systems Containing Rose Bengal and the Cobaloximes of Bfx-Bridged Oxime Ligands. *J. Phys. Chem. C* **2010**, *114*, 15868-15874.
- (64) McCormick, T. M.; Calitree, B. D.; Orchard, A.; Kraut, N. D.; Bright, F. V.; Detty, M. R.; Eisenberg, R. Reductive Side of Water Splitting in Artificial Photosynthesis: New Homogeneous Photosystems of Great Activity and Mechanistic Insight. *J. Am. Chem. Soc.* **2010**, *132*, 15480-15483.
- (65) Guttentag, M.; Rodenberg, A.; Kopelent, R.; Probst, B.; Buchwalder, C.; Brandstaetter, M.; Hamm, P.; Alberto, R. Photocatalytic H-2 Production with a Rhenium/Cobalt System in Water under Acidic Conditions. *Eur. J. Inorg. Chem.* **2012**, 59-64.
- (66) Shan, B.; Baine, T.; Ma, X. A. N.; Zhao, X.; Schmehl, R. H. Mechanistic Details for Cobalt Catalyzed Photochemical Hydrogen Production in Aqueous Solution: Efficiencies of the Photochemical and Non-Photochemical Steps. *Inorg. Chem.* **2013**, *52*, 4853-4859.
- (67) Bachmann, C.; Probst, B.; Guttentag, M.; Alberto, R. Ascorbate as an Electron Relay between an Irreversible Electron Donor and Ru(II) or Re(I) Photosensitizers. *Chem. Comm.* **2014**, *50*, 6737-6739.
- (68) Han, Z.; Qiu, F.; Eisenberg, R.; Holland, P. L.; Krauss, T. D. Robust Photogeneration of H₂ in Water Using Semiconductor Nanocrystals and a Nickel Catalyst. *Science* **2012**, *338*, 1321.
- (69) Das, A.; Han, Z.; Haghighi, M. G.; Eisenberg, R. Photogeneration of Hydrogen from Water Using CdSe Nanocrystals Demonstrating the Importance of Surface Exchange. *Proc. Natl. Acad. Sci. U.S.A.* **2013**, *110*, 16716-16723.

For Table of Contents Only



Synopsis

CoGGH, a Gly-Gly-His tripeptide coordinated to a cobalt ion, is shown to catalyze aqueous proton reduction in a visible light-driven reaction. When coupled with the photosensitizer $[Ru(bpy)_3]^{2+}$ and the sacrificial electron donor ascorbic acid, a reductive quenching mechanism is operative for producing hydrogen (H₂). The evaluation of activity shows that CoGGH is robust, evolving H₂ from water near neutral pH in a long-lived photocatalytic system.